Available online at www.sciencedirect.com

ScienceDirect

Procedia CIRP 75 (2018) 415–420

www.elsevier.com/locate/procedia

15th CIRP Conference on Computer Aided Tolerancing – CIRP CAT 2018

Evaluation of the spring-in of CFRP thin laminates in dependence on process variation

Andrea Corrado, Wilma Polini*, Luca Sorrentino, Costanzo Bellini

Department of Civil and Mechanical Engineering, University of Cassino and Southern Lazio, via G. di Biasio 43, Cassino 03043, Italy

* Corresponding author. Tel.: +39-0776-2993679; fax: +39-0776-2993546. *E-mail address:* polini@unicas.it

Abstract

The cure process of CFRP laminates induces residual stress inside the parts that causes geometrical unconformities. The most important unconformity is the spring-in that means the deviation of the flange-to-flange angle from the design angle. The spring-in value depends on some process parameters, such as the lay-up sequence of the plies, as demonstrated in previous works. The aim of this work is to study the dependence of the spring-in on the deviations in the orientation of the plies due to a hand process. A numerical tool was developed and experimentally tested.

Peer-review under responsibility of the Scientific Committee of the 15th CIRP Conference on Computer Aided Tolerancing - CIRP CAT 2018.

Keywords: Spring-in; Process variation; CFRP laminates

1. Introduction

Composite materials are used in many fields due to their high strength-weight ratio. However, some applications require small geometrical deviations, i.e. high quality requirements, to avoid aesthetical defects or internal residual stresses. Moreover, small geometrical deviations on product single components involve significant geometrical deviations on the entire assembly, as studied in [1,2], that may be in composite or in composite and metallic materials [3]. Geometrical deviations are generally caused by residual stress and deformations due to the cure process and to the thermo-mechanical characteristics of the involved materials [4].

The spring-in is a kind of deviation that can arise during the cure process. It is generally defined as a deviation of the flange-to-flange angle from the nominal value [5] and it is due to many factors, such as the material coefficient of thermal expansion (CTE), the resin chemical shrinkage, the fibre volume fraction gradient and the interaction with the tool.

Resin and fibre have different CTEs and composites plies present a transversely isotropic CTE, but the related stresses do not cause deformations if they are allowed to self-equilibrate. Moreover, the in-plane CTE of the laminate is lower than the through-thickness one and this mismatch causes the spring-in distortion in a curved laminate [6].

The chemical shrinkage of resin is another reason of material distortion because the fibres do not shrink and oppose to the contraction of laminate [7].

Finally, the interaction between the laminate in composite material and the mould during cure process causes distortions [8] because the mould material has usually a CTE higher than composite material [9].

In addition to the described factors, there are other factors, related to the manufacturing process, that can not be ignored, as the curing temperature [10,11], the pressure [12] and the hand lay-up of prepreg [13,14] that influence the spring-in angle of laminates. However, all those studies consider different nominal values of the process parameters, but no one investigate the dispersion around those nominal values.

This work aims to evaluate how the dispersion of the ply orientation around the nominal value influences the geometrical deviation of a composite part: the spring-in. The evaluation of ply orientation angle after the manufacturing process is very hard. Many factors contribute to the deviation of the ply angle from the nominal one [10]. For example, the cut of a piece of unidirectional ply from a tape or from a sheet

2212-8271
Peer-review under responsibility of the Scientific Committee of the 15th CIRP Conference on Computer Aided Tolerancing - CIRP CAT 2018.
10.1016/j.procir.2018.04.042

may involve a misalignment or a waviness in the fibres. Moreover, slight errors can be made in alignment of the tools used to guide cutting. Finally, during the cure cycle the plies are not fully restrained and some movement can occur causing small variations in the ply angle [15–19]. Therefore, the errors in the alignment during the manufacturing process are unavoidable and to control the ply angle with high accuracy is very difficult.

In this study, these factors were considered numerically as a single effect on the accuracy of ply orientation. To investigate this accuracy, the spring-in angles of L-shaped laminates were measured with a coordinate measuring machine (CMM) and the fibres alignment was measured on images acquired by optical microscope.

A numerical tool was developed to simulate the effect of the dispersion in the ply orientation, when they are positioned by hand during manufacturing, on the spring-in of a L-shaped manufactured part. It takes into account the interaction between material characteristics, such as cure kinetics, thermal and mechanical properties, and the boundary conditions, constituted by thermal flows, pressure and mechanical constraints in order to determine the final deformation due to residual stresses. This activity has involved the Monte Carlo method, considering a random ply orientation based on a Gaussian distribution. To discuss the validity of the numerical tool, the experimental and numerical results were compared.

2. Material and method

In this work, a L-shaped part, with squared flanges, whose side is 80 mm and whose corner has a radius of 6 mm, was used as reference case study (see Fig. 1). The composite material considered for this work was Cycom970/T300, a prepreg with a nominal thickness of 0.2 mm, made of unidirectional carbon fibres and epoxy resin with a fibre volume fraction of 60%.

2.1. Numerical tool

The developed numerical model is constituted by three main steps that are identified as 1, 2 and 3 in Fig. 2: definition and pre-processing of the nominal model, generation of the ply misalignment and evaluation of the spring-in. The numerical tool architecture is based on MSC Marc Mentat® solver and Matlab® environment that interact, as shown in Fig. 2.

The first step defines the model to simulate the interaction between material characteristics, such as cure kinetics, thermal and mechanical properties, and the boundary conditions, constituted by thermal flows, pressure and mechanical constraints, in order to determine the final distortion due to the residual stresses.

The simulation model takes into account six prepreg plies laid on U-shaped aluminium mould with $[0°,90°,0°]_s$ lay-up sequence. A 2D mesh, constituted by quad plain strain elements, was used. All physical properties of prepreg and mould are shown in Table 1.

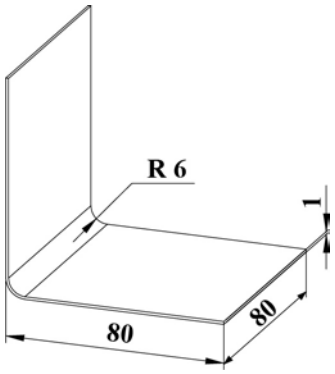

Fig. 1. L-shape part

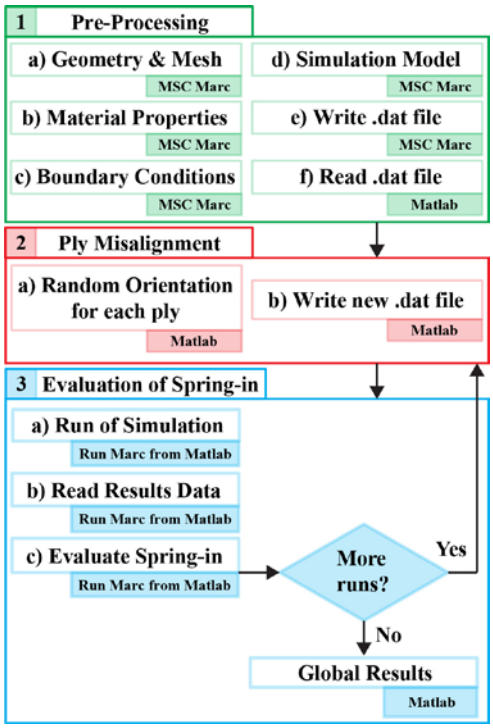

Fig. 2. Process flow of the numerical tool.

This step considers two kinds of analysis: a thermo-chemical analysis to simulate the curing process and a thermo-mechanical analysis to evaluate the residual stresses and related deformations.

The thermo-chemical analysis was based on the energy balance described according to:

$$\rho_c c_{p,c} \frac{\partial T}{\partial t} = \nabla \left(k_c \nabla T \right) + \rho_r V_r \dot{Q} \tag{1}$$

where ρ represents material density, c_p is the specific heat, T is the temperature, t is the time, k is the thermal conductivity coefficient of the composite material, $\dot{Q}$ is heat generation rate of chemical reaction, V is the volumetric percentage. The subscripts f and r refer to fibre and matrix respectively, while c is of composite. Composite density and specific heat can be derived from corresponding properties of raw materials and from volumetric and weight fractions, respectively, through the rule of mixture [20,21].

Table 1. Physical properties of prepreg and mould.

Property of prepreg	Value	Property of mould	Value
Density (kg/m^3)	ρ_f = 1,760; ρ_r = 1,290; ρ_c = 1,572	Density (kg/m^3)	2,700
Specific heat (J/kgK)	$C_{p,c}$ = 1,002	Specific heat (J/kgK)	960
Thermal conductivity (W/mK)	k_{c1} = 4.88; $k_{c2} = k_{c3}$ = 0.51	Thermal conductivity (W/mK)	120
Young's moduli (GPa)	E_{11} = 135; $E_{22} = E_{33}$ = 8	Young's modulus (GPa)	71
Poisson's moduli	υ_{12} = 0.25; υ_{23} = 0.34; υ_{31} = 0.015	Poisson's modulus	0.334
Shear moduli (GPa)	G_{23} = 2.76; $G_{12} = G_{31}$ = 5	CTE	2.4x10^{-7}
CTE (longitudinal)	1.4x10^{-8}		
CTE (transverse)	3.2x10^{-5}		
Total volumetric cure shrinkage	0.0561		
α_{C1}	0.055		
α_{C2}	0.67		
A coefficient	0.173		
Frequency factor	A_c = 0.61		
Activation energy (J/mol)	E = 24,230		
m	0.073		
n	0.82		
Total heat of reaction (J/kg)	H_r = 615,789		

The heat generation rate was evaluated as:

$$\dot{Q} = H_r \left(A_c \exp\left(\frac{E}{-RT} \right) \right) \alpha^m (1-\alpha)^n \quad (2)$$

where H_r is the total heat of reaction, A_c is the frequency factor, E is the activation energy, R is the universal gas constant, α is the cure rate, m and n are the reaction orders. The values was evaluated through Differential Scanning Calorimetry tests according to ASTM E2070 [22].

The thermo-mechanical analysis is a 2D plain strain condition, where the contact between composite material and mould is frictionless and the loads are due to the pressure applied by vacuum bag, to the thermal expansion and shrinkage (described through CTE), and to chemical shrinkage, that can be defined as:

$$\begin{aligned} V_r^S &= 0.0 \quad \text{if} \quad \alpha < \alpha_{C1} \\ V_r^S &= A\alpha_S + \left(V_r^{S\infty} - A\right)\alpha_S^2 \quad \text{if} \quad \alpha_{C1} \le \alpha \le \alpha_{C2} \\ V_r^S &= V_r^{S\infty} \quad \text{if} \quad \alpha \ge \alpha_{C2} \\ \alpha_S &= \frac{\alpha - \alpha_{C1}}{\alpha_{C2} - \alpha_{C1}} \end{aligned} \quad (3)$$

where α_{C1} and α_{C2} are the critical degrees of cure after which the resin shrinkage begins and after which the resin shrinkage stops respectively, α_S is the degree of cure shrinkage, A is a cure shrinkage coefficient and V_r^S is the resin volumetric cure shrinkage.

Once the geometry, the material properties, the boundary conditions and the simulation model were defined, the first step ends with the generation of the file (.dat file) to send to the next step.

The second step generates each ply orientation. The L-shaped part has a nominal lay-up sequence of $[0°,90°,0°]_S$; a random number based on a normal distribution was given for each ply with a mean value μ_{ply} equal to the nominal orientation value of the ply (0° or 90°) and a standard deviation σ_{ply} in order to obtain orientation errors of ±3°, ±6°, ±9° and ±12 °. Once the orientation of each ply is defined, the file to be sent to the next step (new .dat file) is re-generated with this new information.

The third step runs the simulation with MSC Marc solver to evaluate the spring-in value φ after demoulding of component, as shown in Fig. 3. Using the Monte Carlo method, N iterations can be run in order to simulate N stacking of prepreg plies to evaluate N values of spring-in angle that can be described by a mean value μ_φ^{num} and a standard deviation σ_φ^{num}.

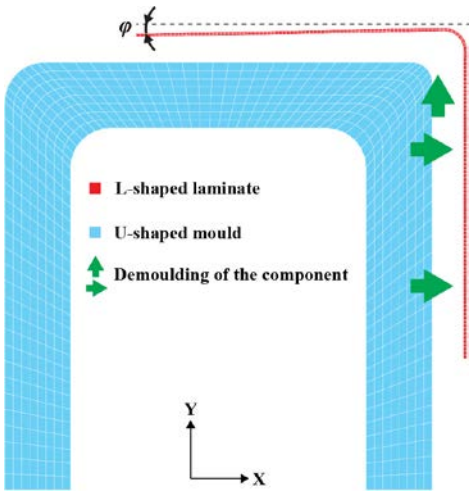

Fig. 3. Spring-in at the end of a simulation run.

2.2. Manufacturing process

Some experimental tests were carried out to validate the numerical model adopted in the present study. To manufacture L-shaped parts, each single hand-cut ply of prepreg was 100 x 200 mm^2 and the hand lay-up of prepreg was carried out on a U-shaped aluminium mould with two corners with radii of 6 mm and 12 mm and maximum dimensions of 380x130x130 mm^3.

Vacuum bag process was used as manufacturing technology to realize, by two batch, four L-shaped parts. A release film was applied over the surface of the mould to easily remove cured parts. Each ply was carefully laid-up on the mould to form a stack with $[0°,90°,0°]_S$ as lay-up sequence. The stack was then covered with a release film and a breather fabric before applying a vacuum bag with the help

of a sealant tape. A vacuum of -10^5 Pa was applied after laying up the parts. Finally, the cure cycle, which consisted of one dwell, was started.

During the heating, the part was heated up to 140°C at 2.5°C/min; once reached, the maximum temperature was hold for 180 min. After cure process, the mould was left to cool down up to the room temperature. At the end of the manufacturing process, a cutting machine with diamond disk was used to trim the edges of the laminates that then were measured by a coordinate measuring machine (CMM) to evaluate the geometrical distortions of the produced parts. Fig. 4 shows the vacuum bagging (a) and the manufactured parts (b).

Fig. 4. (a) Forming process; (b) Manufactured parts.

2.3. Measurement process

A Prismo Vast MPS CMM of Zeiss® was used to measure the flange-to-flange angle of 4 manufactured L-shaped parts in order to evaluate the spring-in. Its volumetric accuracy is 3 μm on one measured meter.

To clamp the L-shaped parts on the CMM and the U-shaped mould, standard trading components and modular elements (by Witte®) were used. The mould surface used for the measurement process included a series of threaded holes in which fast-holding springs and pin locators were coupled. The fast-holding springs were composed by a series of elements, as shown in Fig. 5, and they had the possibility to regulate the position of the fixturing points along the Z-axis, in order to adjust the clamping constraints. The regulation of this position was carried out by screwing (or unscrewing) the screw located in the threaded hole on the mould surface at which a cap nut is connected, as shown in Fig. 5.

Once placed and clamped the L-shaped part on the fixturing equipment, the location of the DRF (Datum Reference Frame) and the measurement strategy were defined. In particular, the measurement strategy was formed by 13-points along 13 lines for a total of 169 points equally spaced at 5 mm on each surface.

The mould was fixed on the measurement surface of CMM and an analogical probe was used to acquire spatial data, whose tip diameter was 3 mm and stylus length was 40 mm.

Moreover, a series of images were acquired by Leica VMM 200 optical microscope with a magnification 50x to which a camera (640x480 pixels) was fixed, in order to evaluate the magnitude of fibre misalignments. In details, data were captured on the corner radius (strategy 1) and on the flanges (strategy 2). Each strategy allowed to acquire images in specific areas indicated by capital letters, as shown in Fig. 6. The alignment of parts was performed by aligning one side of each part with the horizontal line of the viewfinder that it is visible in the optic of the microscope.

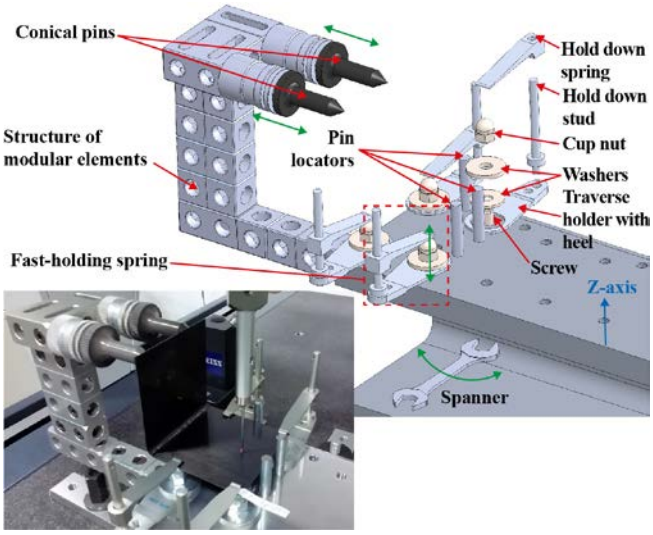

Fig. 5. Clamping system of the L-shaped part during measurement process.

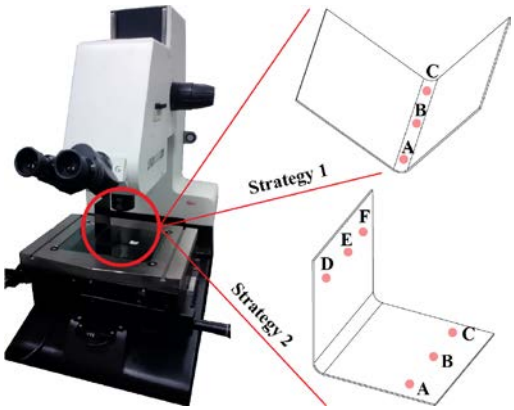

Fig. 6. Optical microscope to evaluate the fibre misalignments.

3. Results and discussion

In this section the results achieved in this study are presented. First of all, the measurement results on spring-in are reported, since they were the input of the numerical model. Therefore, the suitability of the developed model was verified.

3.1. Measurement results

All clouds of points acquired by CMM were elaborated in order to evaluate the deviations from the nominal of the four manufactured parts by means of Zeiss Calypso® software. The results of the measurements show that the mean value μ_{φ}^{exp} of spring-in is equal to 1.09° and the standard deviation σ_{φ}^{exp} is equal to 0.024°. These results were obtained by measuring each part four times, for a total of sixteen placements, sixteen clampings and localizations of DRF. In this way, the measurement uncertainty of 0.006° was also evaluated. The images acquired by Leica VMM 200 optical microscope were analysed. Four red dashed lines were drawn on each image

taken in strategy 1, while only two red dashed lines for the images taken in strategy 2, as shown in Fig. 7. These dashed lines were placed along some fibres in order to evaluate the misalignment of fibres with respect to the reference defined on the examined part.

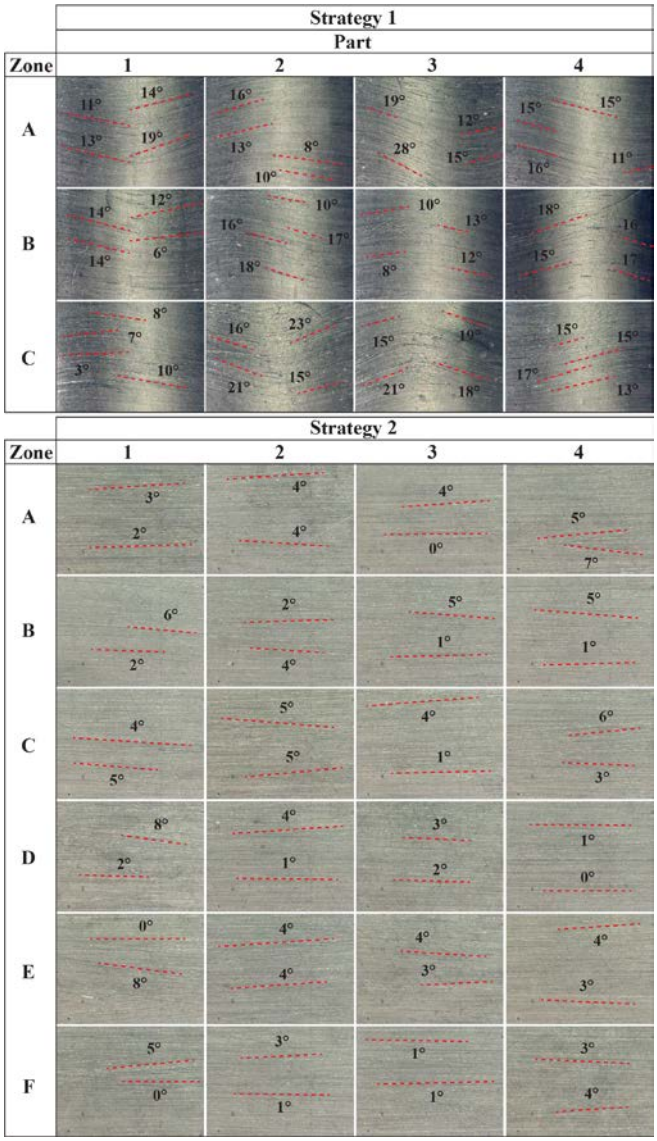

Fig. 7. Images acquired by the optical microscope.

The images taken on the corner radius (strategy 1) show a pronounced waviness in the alignment of fibres with a maximum value of 28°. Otherwise, the images taken on the flanges (strategy 2) show small variations in the alignment of fibres with a maximum of 8°. These results show that the standard deviation of spring-in angle is greatly influenced by the fibre misalignments on the corner radius of the L-shaped parts. The measured angles can be considered as semi-range values. With this hypothesis, the mean of these angles returns an estimation of the alignment error of fibre/ply; this error is about ±8.76°.

3.2. Model validation

First of all, the numerical tool was used to determine a relationship between the standard deviation of the spring-in angle distribution and the standard deviation of the ply orientation distribution. To do this, some simulations were performed by varying the number of Monte Carlo runs (N = 500, 1,000, 1,500 and 2,000) and the standard deviation σ_{ply} of the ply orientation distribution. The values of σ_{ply} were 1°, 2°, 3° and 4°, since those are commonly used industrially.

The simulation results are shown in Fig. 8; they were fitted by means of a third degree regression curve, whose Rsq was 99%:

$$\sigma_{\varphi}^{num} = -0.0007\sigma_{ply}^{3} + 0.0098\sigma_{ply}^{2} - 0.0139\sigma_{ply} + 0.0088 \quad (4)$$

The curve shows how an increase of the standard deviation σ_{ply} of the ply orientation distribution implies an increase of the standard deviation σ_{φ}^{num} of the part spring-in distribution.

Knowing the experimental standard deviation σ_{φ}^{exp} of the spring-in angle distribution and putting it in the equation (4), it is possible to estimate the standard deviation value σ_{ply}^{*} of the ply orientation distribution. Therefore, if the measured standard deviation σ_{φ}^{exp} of the spring-in angle distribution is equal to 0.024°, then the standard deviation σ_{ply}^{*} of the ply orientation distribution is equal to 2.48°.

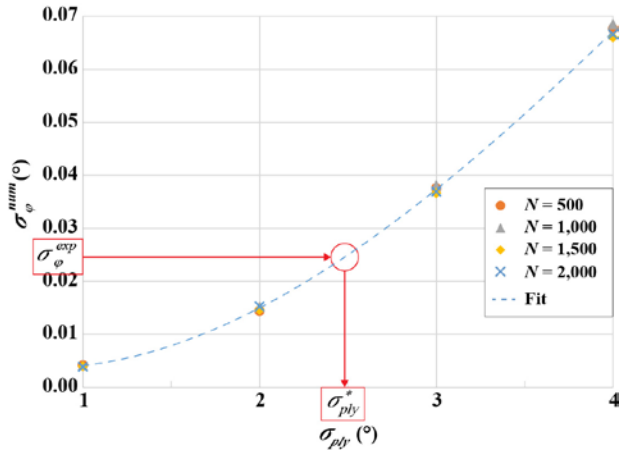

Fig. 8. Relationship between the standard deviations of the part spring-in angle distribution (σ_{φ}^{num}) and of the ply orientation distribution (σ_{ply}).

The obtained value 2.48° was given as input to the numerical tool to estimate the mean value μ_{φ}^{num} and the standard deviation σ_{φ}^{num} of the spring-in angle distribution that were compared to those obtained experimentally (μ_{φ}^{exp} and σ_{φ}^{exp} respectively).

Monte Carlo runs were 10,000 and the obtained results are shown in Fig. 9. It is possible to see that at least 10,000 Monte Carlo runs are required to make asymptotically stable the mean and standard deviation trends. Moreover, these results show that the mean value μ_{φ}^{num} and the standard deviation σ_{φ}^{num} of the spring-in angle are smaller than 0.03% and 0.84% compared to experimental ones respectively. However, the standard deviation σ_{ply}^{*} of the ply orientation distribution is of

about ±7.44° (±3σ) that is near to the result obtained during the measurement process by the optical microscope (±8.76°). Those results confirm that the magnitude of the ply orientation standardized deviation is 2.48°.

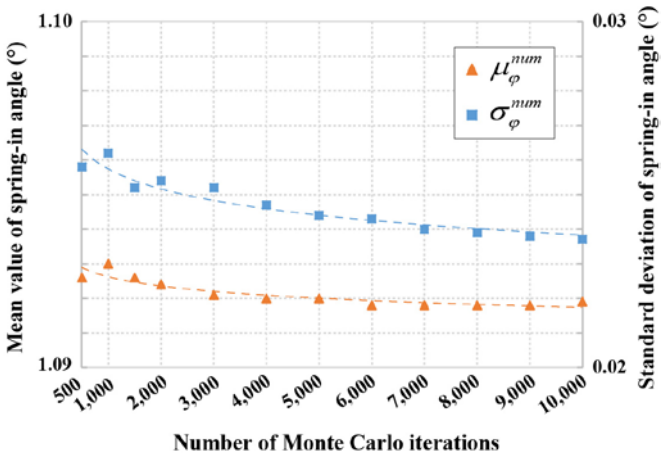

Fig. 9. Mean and standard deviation results of spring-in angle.

4. Conclusions

The cure process of CFRP laminates induces residual stress inside the parts that causes geometrical unconformities as the spring-in. The spring-in value depends by many factors including process parameters, such as the curing temperature, the pressure and the hand lay-up of prepreg. This work aims to study the dependence of the spring-in angle on the deviations in the orientation of the plies due to a hand process.

A numerical tool was developed to foresee the spring-in angle by knowing the ply orientation through three steps: definition and pre-processing of the nominal model, generation of the ply misalignment and evaluation of the spring-in through a Monte Carlo approach. The numerical tool considers a random ply orientation based on a normal distribution with a mean value equal to the nominal orientation value of each ply and a standard deviation equal to about 2.48°. This standard deviation involves a ply orientation error of about ±7.44° (±3σ), that is near to the result of ±8.76° obtained during the measurement process by the optical microscope. It generates a mean value and a standard deviation of the spring-in angle smaller than 0.03% and 0.84% respectively compared to experimental ones.

Further parts and composite materials are matter of further studies to extend the proposed numerical method.

Acknowledgements

This research did not receive any specific grant from funding agencies in the public, commercial, or not-for-profit sectors.

References

[1] Jareteg C, Wärmefjord K, Söderberg R, Lindkvist L, Carlson J, Cromvik C, et al. Variation Simulation for Composite Parts and Assemblies Including Variation in Fiber Orientation and Thickness. Procedia CIRP 2014;23:235–40. doi:10.1016/j.procir.2014.10.069.

[2] Jareteg C, Wärmefjord K, Cromvik C, Söderberg R, Lindkvist L, Carlson J, et al. Geometry Assurance Integrating Process Variation With Simulation of Spring-In for Composite Parts and Assemblies. J Comput Inf Sci Eng 2016;16:31003. doi:10.1115/1.4033726.

[3] Wang H. Investigation on the Effect of Spring-In Distortion on Strength of a Bimaterial Beam. J Aerosp Eng 2016;29:4015069. doi:10.1061/(ASCE)AS.1943-5525.0000566.

[4] Ding A, Li S, Wang J, Zu L. A three-dimensional thermo-viscoelastic analysis of process-induced residual stress in composite laminates. Compos Struct 2015;129:60–9. doi:10.1016/j.compstruct.2015.03.034.

[5] Albert C, Fernlund G. Spring-in and warpage of angled composite laminates. Compos Sci Technol 2002;62:1895–912. doi:10.1016/S0266-3538(02)00105-7.

[6] Mahadik Y, Potter K. Experimental investigation into the thermoelastic spring-in of curved sandwich panels. Compos Part A Appl Sci Manuf 2013;49:68–80. doi:10.1016/j.compositesa.2013.02.006.

[7] Baran I, Cinar K, Ersoy N, Akkerman R, Hattel JH. A Review on the Mechanical Modeling of Composite Manufacturing Processes. Arch Comput Methods Eng 2017;24:365–95. doi:10.1007/s11831-016-9167-2.

[8] Kappel E. Forced-interaction and spring-in – Relevant initiators of process-induced distortions in composite manufacturing. Compos Struct 2016;140:217–29. doi:10.1016/j.compstruct.2016.01.016.

[9] Bellini C, Polini W, Sorrentino L. A new class of thin composite parts for small batch productions. Adv Compos Lett 2014;23:111–6.

[10] Bebamzadeh A, Haukaas T, Vaziri R, Poursartip A, Fernlund G. Response Sensitivity and Parameter Importance in Composites Manufacturing. J Compos Mater 2009;43:621–59. doi:10.1177/0021998308101299.

[11] Bebamzadeh A, Haukaas T, Vaziri R, Poursartip A, Fernlund G. Application of Response Sensitivity in Composite Processing. J Compos Mater 2010;44:1821–40. doi:10.1177/0021998310366062.

[12] Sorrentino L, Bellini C. Compaction influence on spring-in of thin composite parts: Experimental and numerical results. J Compos Mater 2015;49:2149–58. doi:10.1177/0021998314542362.

[13] Hinckley M. Statistical evaluation of the variation in laminated composite properties resulting from ply misalignment. Proc. SPIE 1303, Adv. Opt. Struct. Syst., 1990, p. 497. doi:10.1117/12.21532.

[14] Bellini C, Sorrentino L, Polini W, Corrado A. Spring-in analysis of CFRP thin laminates: numerical and experimental results. Compos Struct 2017;173:17–24. doi:10.1016/j.compstruct.2017.03.105.

[15] Van Dreumel WHM, Kamp JLM. Non Hookean Behaviour in the Fibre Direction of Carbon-Fibre Composites and the Influence of Fibre Waviness on the Tensile Properties. J Compos Mater 1977;11:461–9. doi:10.1177/002199837701100408.

[16] Jumahat A, Soutis C, Jones FR, Hodzic A. Fracture mechanisms and failure analysis of carbon fibre/toughened epoxy composites subjected to compressive loading. Compos Struct 2010;92:295–305. doi:10.1016/j.compstruct.2009.08.010.

[17] Yurgartis SW. Measurement of small angle fiber misalignments in continuous fiber composites. Compos Sci Technol 1987;30:279–93. doi:10.1016/0266-3538(87)90016-9.

[18] Arao Y, Koyanagi J, Utsunomiya S, Kawada H. Effect of ply angle misalignment on out-of-plane deformation of symmetrical cross-ply CFRP laminates: Accuracy of the ply angle alignment. Compos Struct 2011;93:1225–30. doi:10.1016/j.compstruct.2010.10.019.

[19] Thompson SJ, Bichon S, Grant RJ. Influence of ply misalignment on form error in the manufacturing of CFRP mirrors. Opt Mater Express 2014;4:79. doi:10.1364/OME.4.000079.

[20] Blest DC, Duffy BR, McKee S, Zulkifle AK. Curing simulation of thermoset composites. Compos Part A Appl Sci Manuf 1999;30:1289–309. doi:10.1016/S1359-835X(99)00032-9.

[21] Park HC, Goo NS, Min KJ, Yoon KJ. Three-dimensional cure simulation of composite structures by the finite element method. Compos Struct 2003;62:51–7. doi:10.1016/S0263-8223(03)00083-7.

[22] ASTM E 2070. Standard test method for kinetic parameters by differential scanning calorimetry using isothermal methods, 2013. doi:10.1520/E2070.